Assessing general models for the temperature dependence of population density in disease vectors

by

Thomas RC Smallwood
(CID: 01010385)

Supervisors:

Samraat Pawar
Lauren Cator

Department of Life Sciences
Imperial College London
London SW7 2AZ
United Kingdom

A thesis submitted in partial fulfilment of the requirements for the degree of
Master of Science at Imperial College London

Formatted in the journal style of Journal of Ecology

Submitted for the
MSc in Computational Methods in Ecology and Evolution

Acknowledgements

Thanks goes to my supervisors, Samraat Pawar and Lauren Cator, for their invaluable advice and guidance in the completion of the study. I would also like to thank Jonathon Chan, who collated much of the data used in attempting to fit thermal response curves to ecological parameters.

Declaration of Originality

A large portion of the dataset used in the fitting was initially collated and digitised by Jonathon Chan during his undergraduate dissertation, before being added to and standardised by myself. The novel model described and analysed in this study was developed with equal contribution by Samraat Pawar and myself. All other work described here is my own or has been properly referenced.

Copyright Declaration

Contents

List of Tables

List of Figures

Abstract

Vector-borne diseases constitute 17% of the global burden of infectious disease. As the majority of disease vectors are ectotherms life history traits and population density of vectors are highly temperature dependent. This has important consequences for the epidemiology of vector-borne diseases, as vector population is an important ecological parameter in transmission models affecting the encounter rate between vectors and hosts. This study presents a novel mechanistic model of the temperature dependence of vector population density using the Euler-Lotka equation to capture the stage-structured life history of arthropods. This model is compared to a related life history theory-based mechanistic model and a simpler probabilistic model. The two mechanistic models differ in their approach to describing the fecundity schedule of disease vectors, with the novel model using a more complex approach describing the fecundity schedule as a gamma distribution rather than an exponential decay. The functional difference of the probabilistic model is that instead of using a life history theory model based on the Euler-Lotka equation, it incorporates the juvenile life stages of arthropods into a probability of surviving to maturity. Temperature dependence was incorporated into these models using "idealised" thermal response curves to describe the life history parameters. Comparing the thermal response curves predicted by the models shows that the probabilistic models differs greatly from the mechanistic models. The sensitivity analysis indicates this is due to the simplification of the juvenile life stage to a bounded probability, as juvenile life history traits are key parameters in the mechanistic models. This suggests that this simplification fails to capture the important effects of these juvenile stages on the adult vector population density. The thermal response of population density predicted by the two mechanistic models were less different, but indicates that the differing approach to modelling the fecundity does have an important effect on the sensitivity of the model to adult mortality rate. This had a greater influence on the simpler model, due to the presence of additional parameters controlling the fecundity schedule in the novel model. The differences between this selection of models indicates that model choice has a large impact on predictions of thermal tolerance of disease vectors, with important consequences for the incorporation of the temperature dependence of vector population density in epidemiological models.

Keywords
Ecological epidemiology; Life history theory; Mechanistic model; Model sensitivity;

Introduction

Vector-borne diseases are a major global health burden; constituting approximately 17% of the total global burden of infectious disease (WHO, 2004). While malaria is the most prominent vector-borne disease, with 3.4 billion people at risk of the disease, resulting in 198 million cases and 627,000 deaths in 2012 (WHO, 2014), other diseases are also becoming increasingly prominent. Land use change and human population encroachment have been implicated in the 30-fold increase in occurrence of dengue fever between 1960 and 2010 (WHO *et al.*, 2009). Global climate change is also expected to impact on vector-borne diseases (IPCC, 2013) and is implicated in the spread of mosquito-borne diseases including malaria (Gage *et al.*, 2008; Gething *et al.*, 2010; Altizer *et al.*, 2013) and dengue (Hales *et al.*, 2002; Banu *et al.*, 2014). While mosquito-borne diseases are the most studied in this respect, changes in climate are associated with changes in the dynamics of a range vectors and associated diseases (Table 1). In addition to global climate change, food security is expected to be a major challenge of the 21st century in which vectors of plant diseases are an important consideration (Nault, 1997; Childers *et al.*, 2003; Rodrigues *et al.*, 2003; Kitajima *et al.*, 2003). Therefore understanding the ecology of disease vectors is of huge importance and an area of research currently at the forefront of epidemiology.

One approach to investigating the ecology of disease vectors is by developing mechanistic models, in which ecologically meaningful parameters are applied within a framework developed from the underlying biological principles. This is in contrast to empirical models which are simply statistical descriptions of the relationship between the dependent and independent variables. As the parameters in an empirical model therefore have no intrinsic ecological meaning, mechanistic models have the advantage of being more informative. Through a sensitivity analysis it is possible to gain insight into systems defined by mechanistic models by determining how the biological parameters influence the models predictions. This is beneficial in the context of epidemiological models as

Table 1: Examples of vectors affected by changing ambient temperatures under climate change and major associated diseases

Vector	Disease	References
Mosquitoes	Malaria, Yellow fever, Dengue fever, Chikungunya	Gething *et al.* (2010); Banu *et al.* (2014); Campbell *et al.* (2015); Parham *et al.* (2015*a*)
Ticks	Lyme disease, Tularemia	Ogden *et al.* (2014); Ostfeld and Brunner (2015)
Triatominae	Chagas disease	Medone *et al.* (2015)
Sand flies	Leishmaniasis, Bartonellosis, Papataci fever	González *et al.* (2014)
Tsetse flies	Sleeping sickness, Animal trypanosomiasis	Terblanche *et al.* (2008)
Midges	Bluetongue virus	Lysyk and Danyk (2007); Tabachnick (2010)
Fleas	Plague	Purse *et al.* (2006); Gage *et al.* (2008)

it provides insights into the effects of parameters on the population density of vectors and the transmission of diseases, from which the potential efficacy of different forms of vector control and intervention can be assessed.

As the majority of disease vectors are arthropods (Gage *et al.*, 2008; Tabachnick, 2010), and therefore ectotherms, ambient temperature has a large impact on fitness and population growth rate (Savage *et al.*, 2004). This is because, without homoeostatic control of body temperature, metabolic rates in ectotherms are heavily influenced by the ambient temperature (Angilletta, 2009). As a consequence of this thermal dependence, ambient temperature strongly impacts key life history traits such as fecundity, mortality, and development rates in ectotherms (Gage *et al.*, 2008; Dell *et al.*, 2011). The effect of temperature on such traits therefore has a substantial down-stream effect on the population density of disease vectors.

In vector-borne diseases, transmission is strongly affected by the population density of the vector species. This is due to the density dependence of the rate at which infected vectors encounter naïve hosts and at which naïve vectors encounter infected hosts (Gage *et al.*, 2008), with increased vector densities resulting in increased rates of transmission (Kuno, 1995). Reduced density of mosquitoes has therefore been shown to result in declines in malaria burden in Tanzania (Meyrowitsch *et al.*, 2011). Therefore vector population density is a key ecological parameter in many epidemiological models of vector-borne diseases, including the widely used R_0 model of malaria transmission developed by Dietz (1993), in which the the basic reproductive number (Heesterbeek, 1996), R_0, is modelled using the equation:

$$R_0 = \left(\frac{Ma^2 bc \mathrm{e}^{-zEIP}}{Nrz} \right)^{1/2} \tag{1}$$

where M is mosquito vector density, a is the biting rate, bc is vector competence (composed of the probability that a bite by an infective mosquito infects a human and that a bite on an infectious human infects a mosquito), z is the mortality rate of adult mosquitoes, EIP is the extrinsic infective period of the malaria parasite in the mosquito vector, N is the human population density, and r is the rate at which infected humans recover and become immune. As ecological parameters related to humans will not be affected by temperature, humans being endotherms, the vector population density will be a key parameter in determining the temperature dependence of R_0, and therefore transmission rate. Therefore in order to develop an understanding of the ecology of vector-borne diseases it is essential to consider the effect of temperature on vector population density through life history and behavioural traits.

Furthermore, understanding this thermal component of disease vector ecology has important consequences for predicting and addressing the future distribution and burden of vector-borne disease. Under global climate change temperature profiles are predicted to change substantially which, given the effects of temperature on the ecology of ectotherms, will affect the distributions and population densities of disease vectors. Due to the importance of population density of vectors in disease dynamics his is expected to have a large effect on the distribution and transmission rates of vector-borne diseases (Zell, 2004; Gage *et al.*, 2008; Tabachnick, 2010; Parham *et al.*, 2015*a*,*b*). There is already substantial evidence of this in the literature with changing climate associated with changing transmission rate and distributions of vector-borne diseases (Table 1). A more robust understanding of the vector ecology underlying these changes is therefore essential in forecasting the future distributions and burden of vector-borne diseases, and therefore in identifying populations at risk.

In this study I present a general mechanistic model of disease vector population density, referred to as the Smallwood-Pawar model, which applies life history theory to model the temperature dependence of population density from the temperature dependence of key life history traits. The approach used by this model will be assessed by comparing the thermal response curve of vector population density predicted to that predicted by other models. In order to determine the impact of the novel approach to describing the fecundity schedule, the model will be compared to the similar life history theory based model developed by Amarasekare and Savage (2012). The mechanistic life history theory approach employed by the Smallwood-Pawar and Amarasekare-Savage model will also be compared to the probabilistic model developed by Parham and Michael (2010). The models will be compared in three ways:

1. Comparison of the thermal response curves for vector population density predicted by each model;

2. The sensitivity of the thermal response curves predicted by the models to the temperature dependence of life history traits contained in the model;

3. The sensitivity of the thermal response curves predicted by the models to thermal mismatches between life history traits.

Methods and Materials

The population density of disease vectors can be described using life history traits. Parham and Michael (2010) developed a probabilistic model (Equation 2), describing M as a product of mean fecundity, $\bar{b}$, the probability of an individual surviving from the egg life stage to the adult life stage, p_{EA}, the development time, a, and the adult mortality rate, z. This model was substituted into Dietz's (1993) R_0 model (Equation 1) for M by Parham and Michael (2010) and Mordecai *et al.* (2013).

$$M = \frac{\bar{b}\, p_{EA}}{a z^2} \tag{2}$$

While this approach describes vector population density as the product of multiple life history parameters, it does not embed the parameters in a mechanistic framework of how they interact in order to determine the population density of a species. A more mechanistic approach is possible using life history theory to model population density (Amarasekare and Savage, 2012; Amarasekare and Coutinho, 2013; Beck-Johnson *et al.*, 2013; Dommar *et al.*, 2014). This approach allows for the explicit incorporation of stage-structuring of life history, which is important to accurately describing the population dynamics of life stage structured populations, which invariably describes the arthropod species which comprise the majority of disease vectors.

While a range of methods can be employed including matrix models (e.g. Dommar *et al.*, 2014) and systems of ordinary (e.g. Lana *et al.*, 2014) or time-delayed differential equations (e.g. Amarasekare and Coutinho, 2013; Beck-Johnson *et al.*, 2013), this study will focus on the description of the role of life history traits through the application of the Euler-Lotka equation, as employed by Amarasekare and Savage (2012). Age structured populations can be modelled using a transition matrix (Caswell, 1989) in which the top row is the fecundity of an individual in each age class and subsequent rows contain the age-specific survivorship to the next age class. From this matrix the Euler-Lotka equation (Lotka, 1907; Lotka and Sharpe, 1911) can be produced:

$$\sum_{x=1}^{n} \mathrm{e}^{-r_{max}x} l_x b_x \mathrm{d}x = 1 \tag{3}$$

in which r_{max} is the population growth rate, n is the number of age classes, l_x is the probability of surviving to age x, and b_x is the age-specific fecundity. For a large number of age classes, this can be rewritten in a continuous form:

$$\int_{a}^{\infty} \mathrm{e}^{-r_{max}x} l_x b_x \, \mathrm{d}x = 1 \tag{4}$$

where a is the age of first reproduction. Assuming a stable age distribution, the model can be used to calculate the intrinsic growth rate, r_{max}, from the expected reproductive success given by $l_x b_x$.

This approach was used by Amarasekare and Savage (2012) to derive a mechanistic model of population growth rate, r_{max}, by using life history traits to describe l_x, the death rate, and b_x, the birth rate. Assuming a Type III survivorship curve, l_x can be described as an exponential decay determined by the mortality rate, which takes the form:

$$l_x = \mathrm{e}^{-(\bar{z}a + z(x-a))} \tag{5}$$

where z is the adult mortality rate, $\bar{z}$ is the juvenile mortality rate, and a is the development time. b_x was described using a fecundity schedule which assumed the the first reproductive event would be the largest, with fecundity decreasing exponentially from this peak fecundity, b_{pk}, with age, and that the first reproductive event occurred so soon after maturation that it could be modelled as occurring at age a, or the age of maturation. With these substituted into the Euler-Lotka equation and rearranged to solve for r_{max}, this produced the model:

$$r_{max} = -z + \frac{1}{a} \cdot \mathrm{W}[b_{pk} a \mathrm{e}^{((z-\bar{z})a)}] \tag{6}$$

where W[.] is the Lambert's W function, which is implemented in order to solve for r_{max}.

However, the assumptions made with respect to the fecundity schedule may not be generally applicable, nor does it allow for the shape of the fecundity schedule to be temperature dependent, as has been observed in spider mites (Stavrinides and Mills, 2011). Therefore this study proposes a novel mechanistic model in which b_x is modelled as a rescaled gamma distribution controlled by three parameters: the peak fecundity, b_k; the time from age of maturation to age of peak fecundity, v; and the gamma distribution shape parameter, k. The difference in the shape of the fecundity schedules is shown in Figure 1. Substituting this into the Euler-Lotka equation, and rearranging to solve for r_{max} gives the equation, the process behind which is described in further detail in Supplementary Information I:

$$r_{max} \approx \left(\log \left(\frac{\Gamma(k) b_{pk} v}{(zv + k - 1)^k} \right) - a\bar{z} + k - 1 \right) \left(\frac{zv + k - 1}{azv - a + k(v + a)} \right) \tag{7}$$

This contribution of these different parameters to the dynamics of the different life stage is summarised in Figure 2.

In order to convert the population growth rate, r_{max}, into a population density, M, the widely-used equilibrium solution of logistic growth model can be applied, which takes the form:

$$M_t = \frac{M_0 K \mathrm{e}^{r_{max} t}}{K + M_0(\mathrm{e}^{r_{max} t} - 1)} \tag{8}$$

where M_0 is the initial population size, and K is the carrying capacity.

In order to describe the thermal dependence of the population growth rate and therefore population density, thermal response curves describing the temperature dependence of the life history traits can be substituted in where appropriate. While different studies may choose to describe only a subset of ecological parameters as temperature dependent (Lana *et al.*, 2014, e.g.), this study will assume that all of the life history traits are temperature dependent, which is consistent with Parham and Michael (2010), Amarasekare and Savage (2012), and Mordecai *et al.* (2013). Furthermore, the temperature dependence of each parameter is required to assess its influence on the prediction. However, the scaling parameter, k, will not be temperature dependent in this study as it is unclear how this will respond to temperature.

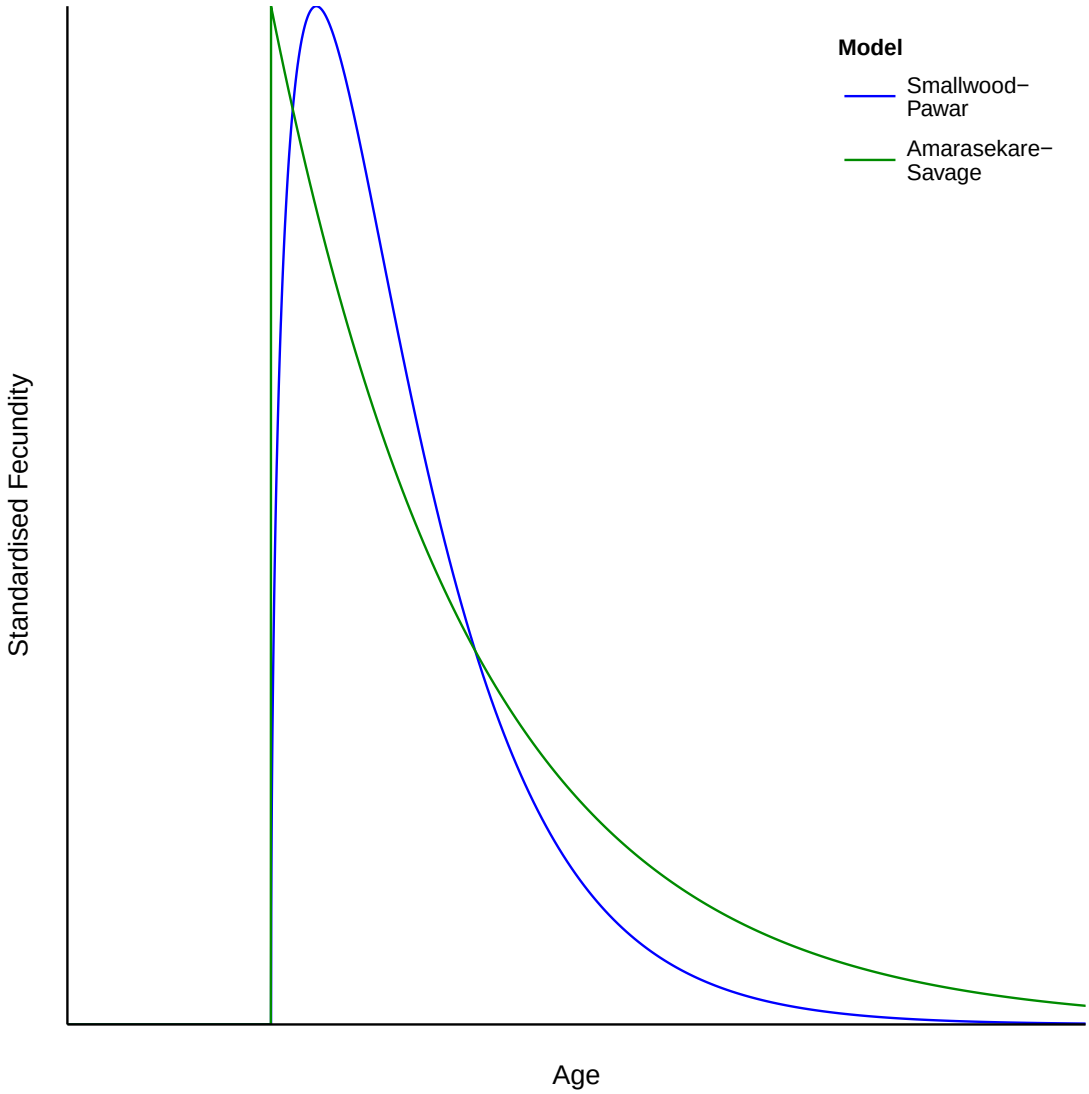

Figure 1: The Amarasekare-Savage model (green) estimates the fecundity schedule of diseases vectors as an exponential decay from peak fecundity which is achieved at the age of maturity. This is compared to the fecundity schedule utilised in the Smallwood-Pawar model (blue) which takes a gamma distribution at which fecundity peaks after a period, v, and is determined by the shape parameter k.

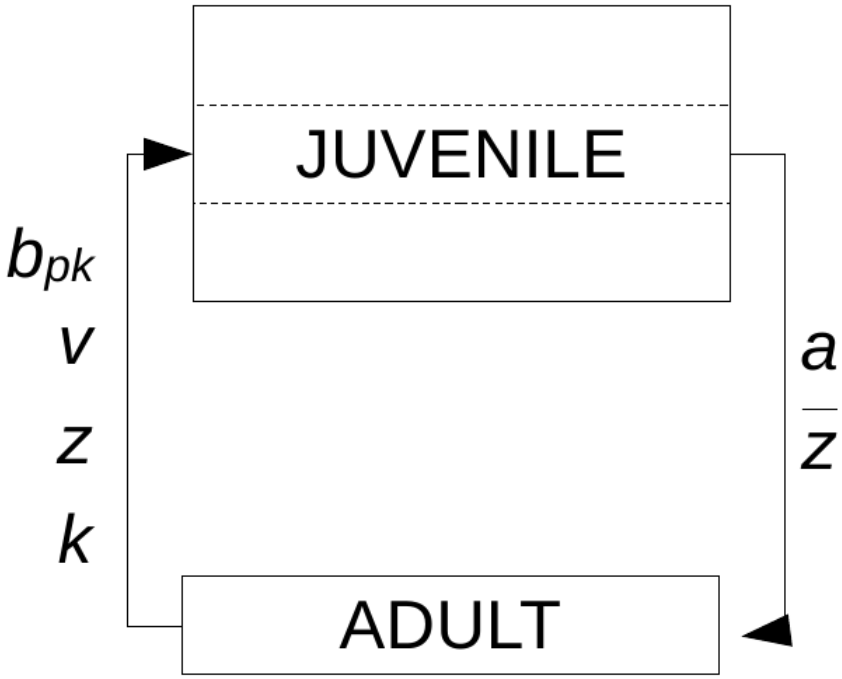

Figure 2: An illustration of how the different factors in the Smallwood-Pawar model impact on the population density of different life stages with the life stages, wiht the vector population density being defined by the adult population density. For simplicity, juvenile stages are collapsed into a single stage with the total development time, a and mean juvenile mortality rate across all juvenile stages, $\bar{z}$, determining the rate at which juvenile enter the adult lifestage from the juvenile to adult life stage. The rate at which offspring are produced by adults is determined by the peak fecundity, b_{pk}, the time between maturation and peak reproduction, v, the adult mortality rate, z, and the fecundity schedule shape parameter, k.

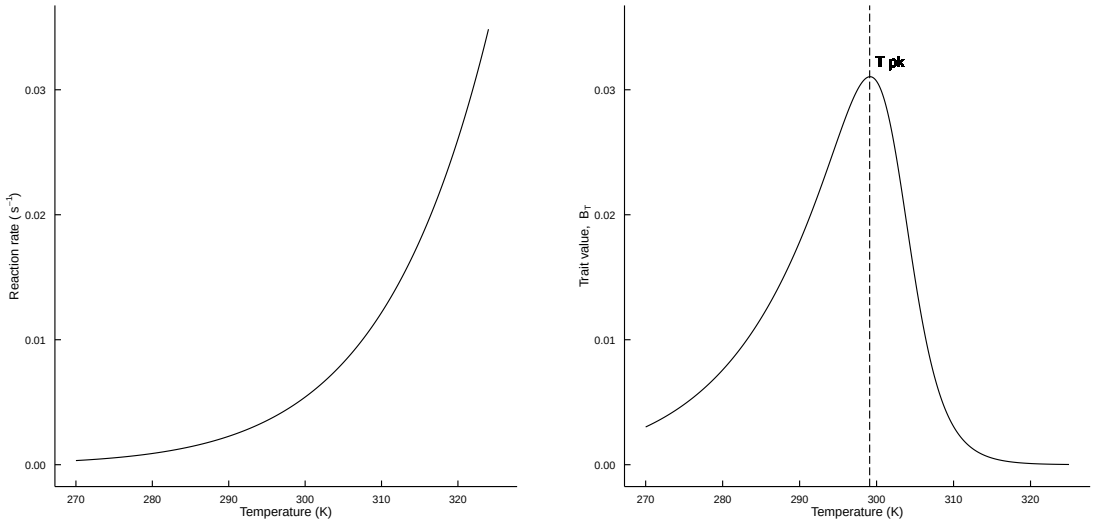

(a) Arrhenius (b) Schoolfield

Figure 3: The Arrhenius model (a) produces an exponential increase in metabolic rate which temperature. However, as metabolism is enzyme-controlled it is expected to follow a unimodal distribution, as are by extension life history traits. This can be captured mechanistically using the Schoolfield model (b).

As the temperature dependence of these life history traits reflects the the temperature dependence of the underlying metabolic rates, the thermal response curves of the life history traits can be modelled as one would model the temperature dependence of metabolism. The temperature dependence of of reaction rates is a well-established principle which can be described by the Arrhenius equation:

$$k = A\mathrm{e}^{\frac{-E_A}{RT}} \tag{9}$$

where k is the reaction rate, A is the prefactor, E_A is the activation energy of the reaction, R is the universal gas constant, and T is the absolute temperature in Kelvin. This predicts an exponential increase in rate of reaction with increasing temperature (Figure 3a). However, in biological systems, reactions are enzyme-controlled. As enzymes are proteins they have narrow range of thermal stability, quickly becoming denatured at temperatures greater than their optimum. As a result biological rates are expected to follow a unimodal function, increasing exponentially to a peak corresponding to an optimal temperature, followed by a rapid decline due to the thermal degradation of the enzymes at high temperatures (Savage *et al.*, 2004). One mechanistic description of this unimodal relationship between temperature and reaction rate was developed by Schoolfield *et al.* (1981) (Figure 3b), with one form of the resulting model being:

$$B_T = B_0 \cdot \frac{e^{\frac{-E_A}{k}\cdot\left(\frac{1}{T}-\frac{1}{283.15}\right)}}{1+\frac{E_A}{E_D-E_A}\cdot e^{\left(\frac{E_D}{k}\cdot\left(\frac{1}{T_{pk}}-\frac{1}{T}\right)\right)}} \tag{10}$$

where the value of trait B_T is determined by the scaling coefficient, B_0, the activation energy, E_A, the deactivation energy, E_D, the temperature in Kelvin at which B_T is maximised, T_{pk}, and the temperature in Kelvin, T.

Table 2: Summary of the life history traits required by each model and their notation and SI units.

Model	Parameter	SI units	Description
Smallwood-Pawar	b_{pk}	offspring female^{-1} s-1	Peak individual reproductive rate
	v	s	Time from maturity to peak reproductiveness
	a	s	Development time
	z	s^{-1}	Adult mortality rate
	$\bar{z}$	s^{-1}	Mean mortality rate across all juvenile life stages
	k		Shape parameter describing the fecundity schedule
Amarasekare-Savage	b_{pk}	offspring female^{-1} s-1	Peak individual reproductive rate
	a	s	Development time
	z	s^{-1}	Adult mortality rate
	$\bar{z}$	s^{-1}	Mean mortality rate across all juvenile life stage
Parham-Michaels	$\bar{b}$	offspring female^{-1} s-1?	Mean individual reproductive rate
	p_{EA}	None	Egg to adult survival probability
	a	s	Development time
	z	s^{-1}	Adult mortality rate

In order to determine the value of the Smallwood-Pawar model (Equation 7) it must be considered in the context of alternative approaches to modelling the population density of disease vectors. Central to the value of this new approach is a comparison to the thermal response curve predicted by the closely related Amarasekare-Savage model (Equation 6) which, as discussed above, applies a similar life-history approach but differs in the description of the fecundity schedule. Comparing the novel Smallwood-Pawar and Amarasekare-Savage models can therefore highlight the impact of differing description of fecundity schedule on predictions of population density, through the increased number of parameters (Table 6). From this it will be possible to draw conclusions as to the effect of the simplifying assumptions made by Amarasekare and Savage (2012) with the respect to the fecundity schedule. The mechanistic approach using life history theory applied by the Smallwood-Pawar and Amarasekare-Savage models are also to be compared to the probabilistic Parham-Michaels model (Equation 2), the parameters of which are also summarised in Table 6.

Model Parametrisation

A dataset of thermal responses of ecological traits for a range of disease vectors was intended to be used to parametrise the models, however the data proved to not be of sufficient quality to produce thermal response curves which could reliably be utilised in the models of interest, the process and results of which are described in Supplementary Information II.

Instead, "idealised" curves were used for each temperature dependent parameter in the models. The Schoolfield model (Equation 10) of thermal dependence was used as it produced a unimodal thermal response curve as described by Dell *et al.* (2011). While other studies (Mordecai *et al.*, 2013, e.g.[) has used the similar, unimodal Briere model, the Schoolfield model was selected for this study as one form contains an explicit parameter describing the temperature at which the trait is maximised, T_{pk}, which can therefore be manipulated in order to study the sensitivity of each model to variation in the optima of individual life history traits.

The parametrisation of the Schoolfield model with respect to each life history trait was informed by a review of the relevant literature, including that in the dataset used in the fitting of thermal response models to ecological traits of disease vectors described in Supplementary Information II. From this it was established that 10°C and 40°C were appropriate maximum and minimum temperatures for the thermal response curve. 26°C was determined to be appropriate for the thermal optima of the life history traits, T_{pk}, based on the literature review and it's widespread use as the temperature at which arthropods are raised under experimental conditions. In order to for the different parameters to have the same sensitivity to temperature the activation energy and deactivation energy parameters in the Schoolfield model, E_A and E_D respectively, were identical for all thermal responses and set as 1.7 and 4.5 respectively, values which were determined to result in the trait value to approach 0 at the thermal extremes, 10°C and 40°C. This prevents any difference in the sensitivity of the models to different parameters being due to the differing shape of the thermal response curve. The scaling coefficient for each life history trait, B_0, was set such that the optimum value of the thermal response curve was consistent with the optimal values of the traits reported in the literature, and is reported in Table 3. In the case of life history traits for which the optimum value in as small as possible as opposed to as large as possible, such as the adult and juvenile mortality rate, the development time and the time from age of maturity to peak reproduction, the Schoolfield model was inverted. With respect to development time and time from age of maturity to peak reproduction the meant that they were instead modelled as rates, which is more fitting for the Schoolfield model. For the mortality rates, the uninverted Schoolfield model in fact describes the thermal dependence of longevity. Some estimations also had to be made for life history traits which are not standard traits measured in the literature.

As peak fecundity is not an ecological parameter found in the literature, it was estimated as being approximately equal to the mean fecundity as the fecundity schedule of disease vectors is assumed to be so peaked that the mean fecundity will be dominated by the peak value (Amarasekare and Savage, 2012). Similarly, the time between age of maturation and peak reproduction, v, had to be parametrised given certain assumptions. This was estimated as being approximately equal to the inverse of oviposition rate, or the time between ovipositions, as it was assumed that the first reproductive event would be the largest (Amarasekare and Savage, 2012) and that the oviposition rate does not change with age. The thermal response curve for each parameter is shown in Figure 4.

The thermal response of the shape parameter for the fecundity schedule, k, was for the purposes of this study set as being temperature independent as there was little experimental data from which the shape of the temperature dependence of k could be deduced. k was therefore parametrised with the constant value of 2, which was deemed to produce a suitable model of the fecundity schedule for the purposes of investigating the degree to which this approach would predict a different thermal response curve to that applied in the Amarasekare-Savage model.

As the thermal response curves for the life history traits are not being utilised to make specific predictions but rather to determine the deviation between the predictions of the models and their respective sensitivity and the same idealised curves will parametrise each model, the accuracy of the curves is not as important as the consistency of the curves between parameters and models.

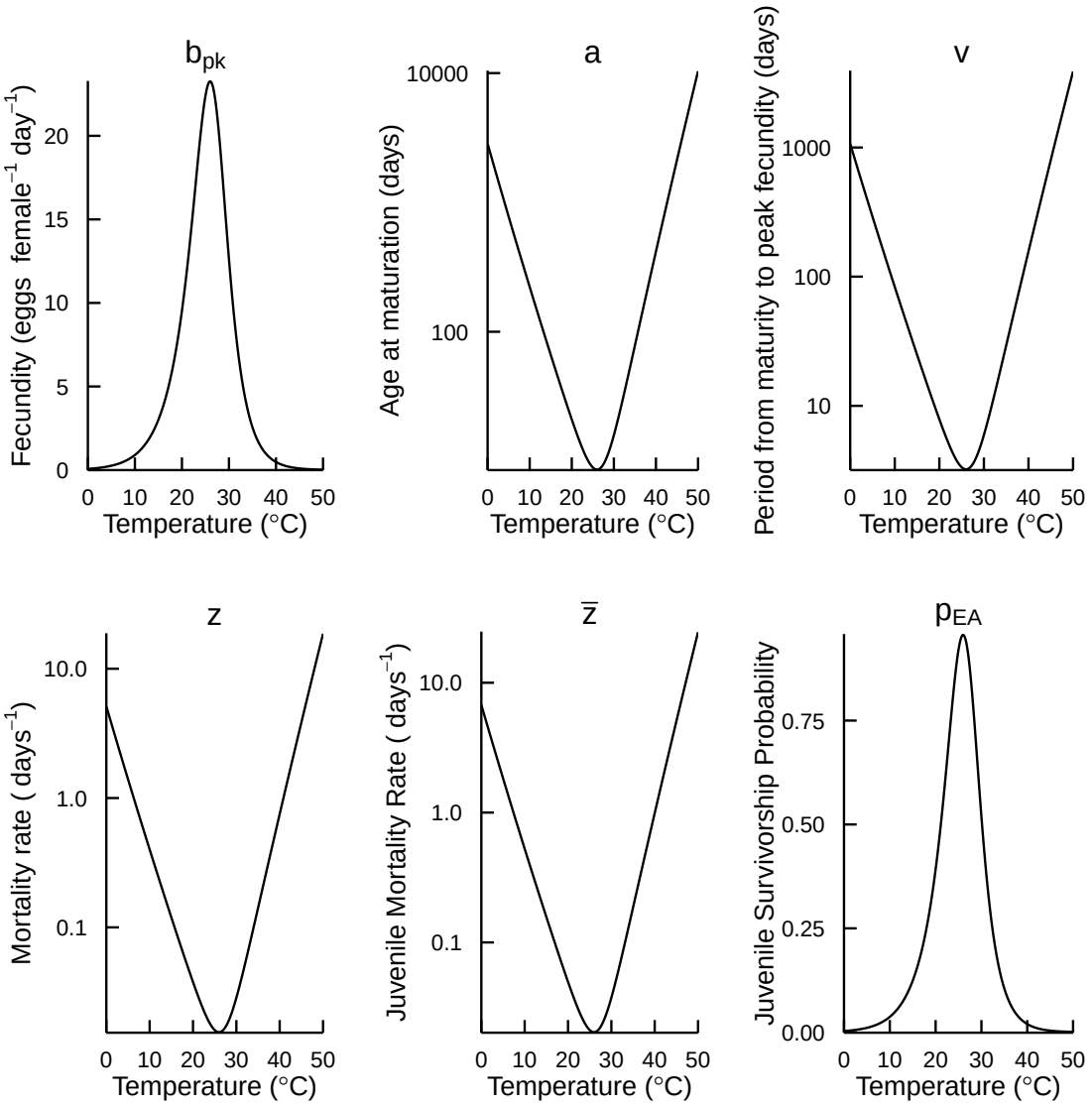

Figure 4: "Idealised" thermal response curves for the key life history traits required by the vector popualtion density models, determined using the Schoolfield model. In order for the temperature dependence of to be equal so as to not weight the sensitivity of the models, each Schoolfield model was parametrised with the same optimum temperature, T_{pk}, and activation and deactivation energies, E_A and E_D. The scaling parameters, B_0, was varied according so the curve is constant with the optimal trait values reported in the literature. As the optimum for development time, mortality rates and time from age of maturity to peak fecundity are a minimum rather than a maximum value, these are parametrised with an inverted Schoolfield model.

Table 3: Summary of the parameter values used in the Schoolfield model to create the thermal response curves for each life history trait contained in the three models. In order to produce curve which have a consistent shape, T_{pk}, E_A and E_D are kept constant between traits, with only B_0 allowed to vary in order to correctly scale the parameters.

Model parameter	Curve parameter			
	B_0	T_{pk}	E_A	E_D
b_{pk}	0.900	26	1.7	4.5
v	0.012	26	1.7	4.5
a	0.005	26	1.7	4.5
z	2.500	26	1.7	4.5
$\bar{z}$	1.900	26	1.7	4.5
p_{EA}	0.037	26	1.7	4.5

Model Comparison

These idealised curves were subsequently input into the models, and the predicted thermal response curves were compared both quantitatively and qualitatively. Quantitative comparisons were made by comparing the predicted thermal optima of the response curves and the shape of the curve. The thermal optima were estimated numerically by finding the maximum value of the temperature dependent population density, M_{pk}, and the associated temperature value, T_{pk}. The shape of the curve was quantified by calculating the temperature range at which temperature dependent population density is predicted to be greater than 80%, referred to as M_{80}. This reflects the thermal tolerance of the predicted thermal response curve near to the optimum which was deemed to be the region of the curve of greatest importance within the context of vector populations,as this constituted to window within which at is expected a population viably act as a reservoir for a vector-borne disease.

Sensitivity Analysis

Due to the complexity of the mechanistic Smallwood-Pawar and Amarasekare-Savage models, it was not possible to apply an analytical approach in the sensitivity analysis, such as that carried out by Mordecai *et al.* (2013), as it was not possible to calculate the partial differentials for each parameter. Their approach used the fact that the derivative of the temperature dependence of population density predicted model can be described as the sum of the partial derivatives of each parameter in the model with respect to temperature, as depicted with respect to the Smallwood-Pawar model in Equation 11. From these partial derivatives it is therefore possible to determine the relative contribution of the temperature dependence of each parameter to the thermal response curve of population density predicted by the model.

$$\frac{\mathrm{d}M}{\mathrm{d}T} = \frac{\partial M}{\partial b_{pk}}\frac{\mathrm{d}b_{pk}}{\mathrm{d}T} + \frac{\partial M}{\partial v}\cdot\frac{\mathrm{d}v}{\mathrm{d}T} + \frac{\partial M}{\partial a}\frac{\mathrm{d}a}{\mathrm{d}T} + \frac{\partial M}{\partial z}\frac{\mathrm{d}z}{\mathrm{d}T} + \frac{\partial M}{\partial b_{pk}}\frac{\mathrm{d}b_{pk}}{\mathrm{d}T} + \frac{\partial M}{\partial b_{pk}}\frac{\mathrm{d}b_{pk}}{\mathrm{d}T} + \frac{\partial M}{\partial \bar{z}}\frac{\mathrm{d}\bar{z}}{\mathrm{d}T} + \frac{\partial M}{\partial k}\frac{\mathrm{d}k}{\mathrm{d}T} \quad (11)$$

However, as this approach was not deemed to be possible an alternative numerical approach was applied. The effect on the population density of the temperature dependence of the parameters in each model was determined by describing each in turn as temperature independent and therefore a constant. As the partial derivative with respect to temperature of a temperature independent parameter is 0, the derivative of this curve would be the sum of the partial derivatives of the temperature dependence of the other parameters. Therefore the deviation of a curve in which one parameter is temperature independent from the fully temperature dependent model will reflect the relative contribution of the temperature dependence of that parameter to the thermal response curve predicted by the model. This can be used to assess the sensitivity of the model to individual parameters as the most influential parameters will be those with the highest relative contribution to the temperature dependence of the model prediction, and therefore the greatest deviation when temperature independent.

This temperature independence of each life history trait was parametrised as being 80% of the optimum trait value. By calculating the constant for each parameter consistently in this way it is possible to directly compare the magnitude of the change in the prediction when each is held constant. The deviation of a thermal response curve where one parameter is temperature independent from the fully temperature dependent model was assessed quantitatively by calculating the change in the optimum temperature, T_{pk}, in the population density at the optimum, M_{pk}, relative to the fully temperature dependent model, and in the thermal range at M_{80}.

Sensitivity of the model to the temperature dependence of the ecological parameters was also determined by assessing the impact of the thermal optima, T_{pk}, of each parameter on the predicted temperature of optimal population density. This was done by varying the T_{pk} of the idealised curve for each parameter between 20°C to 30°C, a range which was determined to be biologically appropriate. At increments of 0.1°C, the thermal response curve for population density was modelled and the optimum temperature, T_{pk}, was recorded. The change in the predicted thermal optimum of population density was plotted against the difference in the thermal optimum of the varied parameter to that of the unvaried parameters, which were kept constant at 26°C, such that the slope of the line described the effect of the change in the optimum temperature of a given parameter on the temperature of optimum population density.

Results

Model Comparison

The three models of population density of disease vectors all predicted the same optimum temperature (T_{pk}) of 26°C, matching the optimum temperature of all the parameters described with a unimodal thermal response curve. However, there was a substantial difference between the shapes of the predicted thermal response curves of population density. The mechanistic Smallwood-Pawar and Amarasekare-Savage models both predict a much broader curve than the probabilistic Parham-Michaels model (Figure 5), as indicated by greater range of the M_{80} values detailed in Table 4. While the shape of the predicted curves differed to a lesser extent between the two mechanistic models, the Smallwood-Pawar model produced a broader thermal tolerance near the optimum, indicated by the greater temperature range at M_{80} (Table 4), but the more significant hump of the Amarasekare-Savage model seen in Figure 5 resulted in it becoming broader further from the optimum.

Table 4: Summary of key shape parameters of the thermal response curves predicted by each model of vector population density. The large difference between the M_{80} ranges of the mechanistic Smallwood-Pawar and Amaraksekare-Savage models from the probabilistic Parham-Michaels model indicates a large difference in the shape of the thermal response curves.

Model	T_{pk}	M_{80} (range)
Smallwood-Pawar	26°C	$20.5 - 30.7$°C (10.2°C)
Amarasekare-Savage	26°C	$21.4 - 30.0$°C (8.6°C)
Parham-Michaels	26°C	$24.9 - 27.0$°C (2.1°C)

Sensitivity Analysis

The temperature dependence of adult mortality was found to have a greater impact on the predictions of the Parham-Michaels model than the thermal dependence of the other parameters, as indicated by the largest change in both the relative peak population density, M_{pk}, and the range of M_{80} values (Table 5), which is also reflected in Figure 6c.

For the mechanistic Smallwood-Pawar and Amarasekare-Savage models the development time, a had the greatest impact on both the relative peak population density, Mpk, and range of M_{80} values (Table 5). However, a qualitative appraisal of the predictions indicates that the temperature dependence of a largely affects the predicted thermal response curve near the optimum, and that juvenile mortality rate, $\bar{z}$, has a greater impact at extreme temperatures in both the Smallwood-Pawar and the Amarasekare-Savage models (Figures 6a and 6b). However, the mechanistic models do differ in their sensitivity to adult mortality, which can be qualitatively determined to also have a large impact on the prediction of the Amarasekare-Savage model (Figure 6b), but little influence on the Smallwood-Pawar model (Figure 6a).

Varying thermal optima of the response curves of the life history traits was found to affect the optimum of the thermal response curve of population density predicted by the Parham-Michaels model. The trait which has the greatest effect, as indicated by the greater slope of the line in

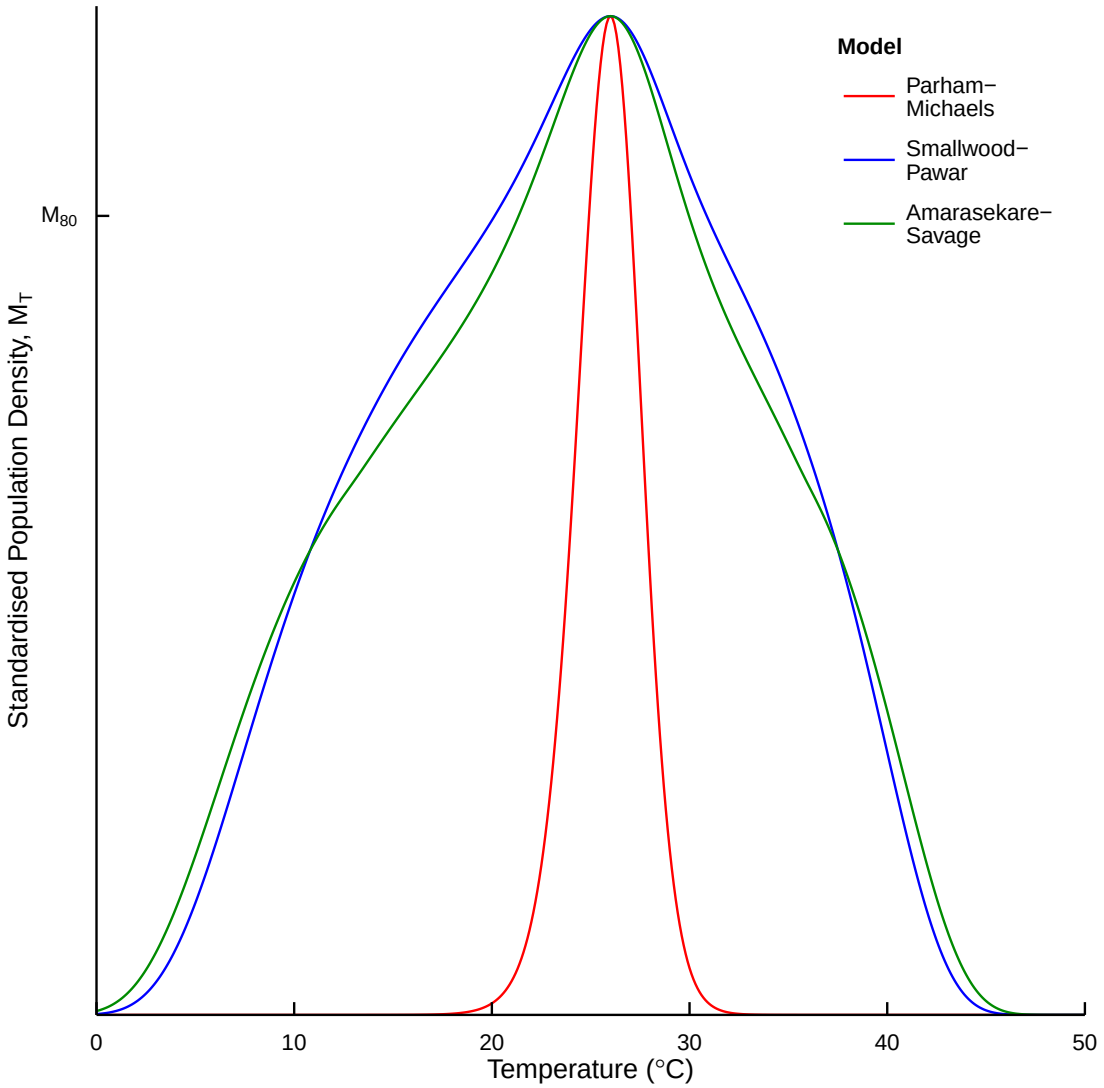

Figure 5: The thermal response curves for population density predicted by each model from the idealised curves describing the temperature dependence of key life history traits. While the curves predicted by the mechanistic Smallwood-Pawar and Amarasekare-Savage models are similar, the probabilistic Parham-Michaels prediction is far narrower indicated a small thermal tolerance.

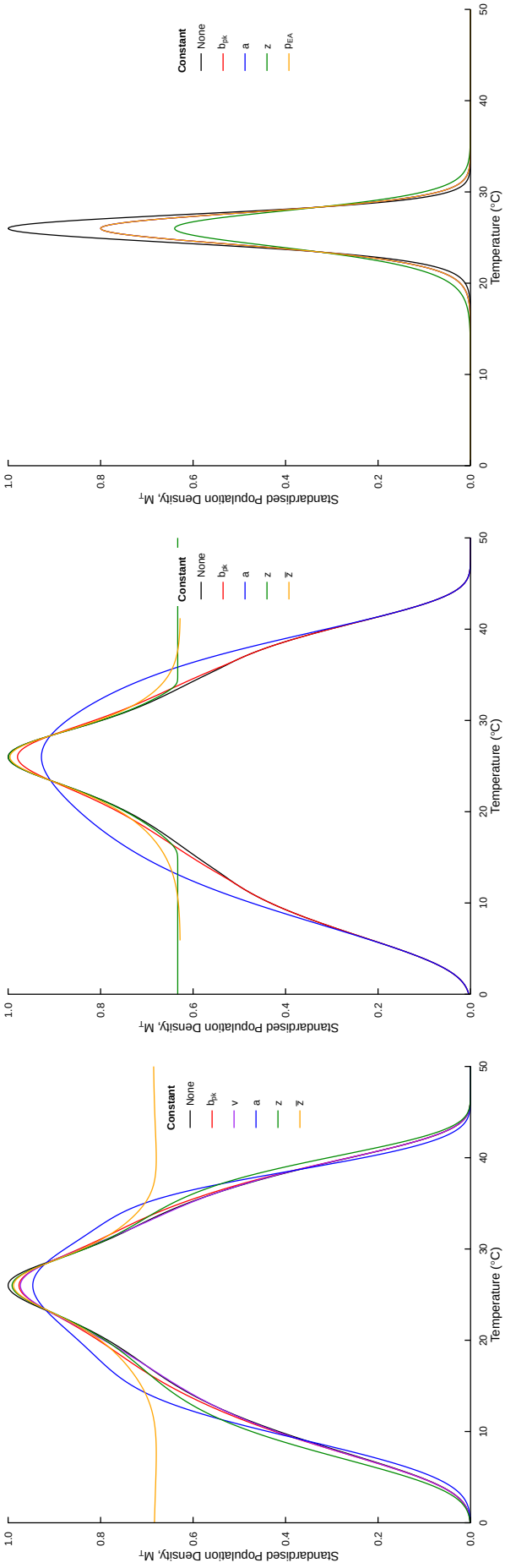

(a) Smallwood-Pawar Model (b) Amarasekare-Savage Model (c) Parham-Michaels Model

Figure 6: Graphs indicating the change in the thermal response curve predicted by each model in response to individual parameters being defined as temperature independent and therefore the sensitivity of each model to the temperature dependence of key life history traits. From this it can be deduced that near the optimum the Smallwood-Pawar and Amarasekare-Savage models are most sensitive to the development time, a, but become highly sensitive to the juvenile mortality rate, $\bar{z}$, at highly suboptimal temperatures. The Amarasekare-Savage model differs from the Smallwood-Pawar model by also being highly sensitive to the adult mortality rate, z, at highly suboptimal temperature. The Parham-Michaels model is determined to be most sensitive to adult mortality rate at all temperatures.

Table 5: Summary of statistics indicating the change in the thermal response curves of each model when individual life history traits are defined as temperature independent, with a larger change relative to other parameters in a model indicating greater sensitivity of the model to the trait held constant. This indicates that the mechanistic Smallwood-Pawar and Amarasekare-Savage models are most sensitive to development time, a, whereas the probabilistic Parham-Michaels model is most sensitivy to adult mortality rate, z.

Model	Parameter	M_{pk}	M_{80} (range)	ΔM_{80} range
Smallwood-Pawar	b_{pk}	0.983	$19.5 - 31.4$°C (11.9°C)	1.7°C
	v	0.988	$20.2 - 30.9$°C (10.7°C)	0.5°C
	a	0.949	$16.6 - 33.6$°C (17.0°C)	6.8°C
	z	0.999	$20.4 - 30.8$°C (10.4°C)	0.2°C
	$\bar{z}$	0.997	$20 - 31.0$°C (11.0°C)	1.4°C
Amarasekare-Savage	b_{pk}	0.980	$20.6 - 30.6$°C (10.0°C)	1.4°C
	a	0.928	$16.1 - 33.8$°C (17.7°C)	10.1°C
	z	0.999	$21.3 - 30.0$°C (8.7°C)	0.1°C
	$\bar{z}$	0.996	$21.1 - 30.2$°C (9.1°C)	0.5°C
Parham-Michaels	b_{pk}	0.80	$24.8 - 27.2$°C (2.4°C)	0.3°C
	a	0.800	$24.8 - 27.2$°C (2.4°C)	0.3°C
	z	0.640	$24.6 - 27.3$°C (2.7°C)	0.6°C
	$\bar{z}$	0.800	$24.8 - 27.2$°C (2.4°C)	0.3°C

Figure 7c, was adult mortality rate, z. The thermal optima predicted by the Smallwood-Pawar and Amarasekare-Savage models were also affected affected by the thermal optima of the life history traits (Figures 7a and 7b). For both of the mechanistic models, the development time, a, was indicated to be the most important parameter determining the peak, as the slope of the line was greatest for this trait. However, as the difference from the reference temperature of 26°C increases Figures 7a and 7b indicated a substantial downwards curve of the line representing the effect of juvenile mortality rate, $\bar{z}$, and therefore an increasing relative influence on the thermal optima prediction of both models.

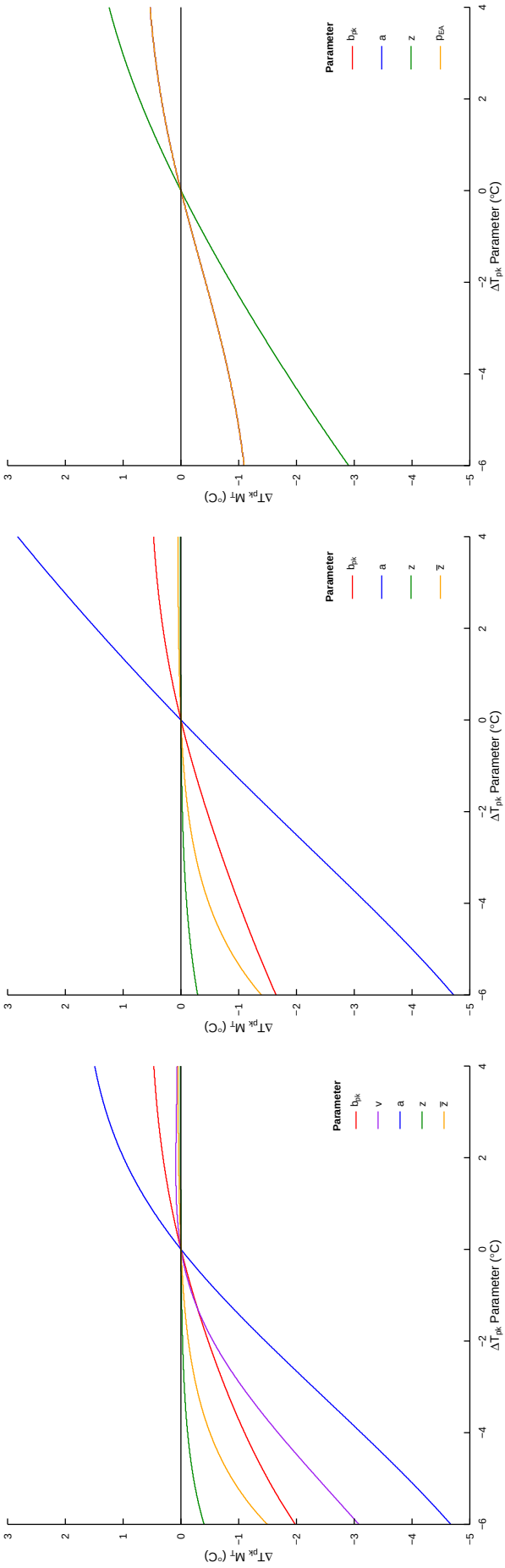

(a) Smallwood-Pawar Model

(b) Amarasekare-Savage Model

(c) Parham-Michaels Model

Figure 7: Sensitivity analysis plots visualising the impact of varying the optimum temperature, T_{pk}, of individual parameters on the thermal optimum predicted by each model. This indicates that the thermal optimum of population density predicted by the Smallwood-Pawar and Amarasekare-Savage models is most sensitive to the optimal temperature for development time, a, whereas the Parham-Michaels model is most sensitive to adult mortality rate, z. The relative importance of juvenile mortality rate in the Smallwood-Pawar and Amarasekare-Savage model can also be seen to increase as the difference in optima increases.

Discussion

Comparing the model predictions in Figure 5, there is a clear difference between the predictions of the probabilistic Parham-Michaels model and the mechanistic Smallwood-Pawar and Amarasekare-Savage models. While the optimum temperatures is 26°C for all three models, this is to be expected as all the ecological parameters used in each model have the same thermal optimum of 26°C. The shape, and therefore the M_{80} temperature range (Table 4), of the models differs however. The thermal response curve of vector population density predicted by the probabilistic Parham-Michaels model is substantially narrower than that predicted by the mechanistic Smallwood-Pawar and Amarasekare-Savage models. By comparison, the difference in shape between the two mechanistic models is far smaller.

That the Smallwood-Pawar and Amarasekare-Savage models produce similar thermal response curves is expected as the approach used in each is very similar, with the most important difference being the approach to modelling the fecundity schedule. However, it is important to assess the degree to which this difference affects the model prediction. The thermal response curve predicted by the Amarasekare-Savage model is narrower near the thermal optimum than that predicted by the Smallwood-Pawar model, as can be seen in Figures 6b and 6a respectively, and deduced from the narrower range at M_{80} (Table 5). However, while both curves show a degree of inflection this is far more prominent in the prediction of the Amarasekare-Savage model, resulting in it being broader at the base than the curve predicted by the Smallwood-Pawar model. This difference in shape may be due to the difference in modelling the fecundity schedule, resulting in the additional life history parameters interacting with some aspect of the model to dampen the inflection. However, the models also differ in the methods employed to estimate r_{max} for the Euler-Lotka Equation (4), with the Smallwood-Pawar model applying a Taylor power expansion and the Amarasekare-Savage model using a Lambert's W function.

The results of the sensitivity analysis suggest that the difference in shape may be due t the difference in the sensitivity of the models to adult mortality rate, as the Amarasekare-Savage model (Figure 6b) was determined to be far more sensitive to this life history parameter at temperatures away from the thermal optimum than the Smallwood-Pawar model (Figure 6a). Furthermore, the increase in sensitivity of the model to adult mortality as the difference in temperature from the optimum increases coincides with the inflection of the curve. One way in which the different approaches to modelling the fecundity schedule may result in the difference in sensitivity of the predicted population density to adult mortality, and therefore the difference in the shape of the curve, is by affecting the influence of adult mortality rate on reproductive output. Adult mortality may only have a large effect on the prediction of population density at highly sub-optimal temperatures because it is only at these temperatures that mortality rate has a large impact on the reproductive output. This is the result of the assumption in the Amarasekare-Savage model that fecundity decays exponentially, resulting in a low level of mortality having little impact as the majority of reproduction occurs soon after maturation. It is only at highly suboptimal temperatures that the mortality rate is high enough to result in a significant proportion of individuals having greatly reduced total fecundity and affecting the birth rate and therefore the population growth rate and density. However, the different approach to modelling the fecundity applied in the Smallwood-Pawar model results in the model being less sensitive to adult mortality as it incorporates a period between the age of maturity and the age of peak reproduction which also increases at sub-optimal temperatures. The increase in age of peak fecundity which results for the increase

in the time between maturity and peak fecundity at sub-optimal temperatures means that the temperature dependence of adult mortality rate alone does not determine the impact of mortality on the fecundity schedule. This therefore reduces the sensitivity of the Smallwood-Pawar model to adult mortality rate.

While the Smallwood-Pawar and Amarasekare-Savage models differ in their sensitivity to adult mortality rate, they are more similar in their sensitivity to the other shared parameters. The temperature dependence of development time, a, has the greatest contribution to the predicted temperature dependence of population density in both the Smallwood-Pawar and Amarasekare-Savage models based on the relative M_{pk} and the change in the temperature range at M_{80} (Table 5), and can be seen in Figures 6a and 6b. While the magnitude of the change is slightly greater for the Amarasekare-Savage model (Relative $M_{pk} = 0.928$ and change in M_{80} range = 10.1°C, compared to 0.949 and 6.8°C; Table 5), this is likely due to the lower number of parameters in the model compared to the Smallwood-Pawar model, resulting in the temperature dependence of each individual having a higher contribution to the temperature dependence of the model prediction. This is supported by Figures 7a and 7b, which indicate that the thermal optimum of the predictions of response curve of population density is strongly influenced by the thermal optimum of the thermal response curve describing the temperature dependence of development time, a, indicated be the slope of the relationship between change in optimum compared to that of other parameters.

However, while development time,a, is the most important parameter near to the optimum, both the Smallwood-Pawar and the Amarasekare-Savage models are more sensitive to juvenile mortality rate, $\bar{z}$, at highly sub-optimal temperatures (Figures 6a and 6b). This can also be inferred from Figures 7a and 7b, in which juvenile mortality can be observed having an increasingly strong effect on the thermal optimum of the predicted population density of each model from the curve of the relationship. The importance of both development time, a, and juvenile mortality rate, $\bar{z}$, indicates that the mechanistic approach common to these models is highly influenced by the juvenile survivorship which is determined by these parameters (Figure 2). The importance of the dynamics of the juvenile stage may be expected to be important in the population dynamics of disease vectors as they invest in high fecundity soon after maturity before high rate of adult mortality can impact their reproductive output (Amarasekare and Savage, 2012).

The Parham-Michaels model, on the other hand, is most sensitive to adult mortality rate, z. However, as the Parham-Michaels is a probabilistic model this is only informative in terms of how the life history parameters affects the model prediction, rather than providing any basis for a hypothesis as to its role in affecting disease vector population density. Whereas the importance of adult mortality rate in the Amarasekare-Savage model provided insight on the modelling of the fecundity schedule, its importance in the Parham-Michaels model simply reflects that z occurs twice in the model, by virtue of being squared, compared the once of other parameters, resulting in the change in M_{80} range being double that of the other parameters. The relative M_{pk} is also 0.64, the square of the temperature independent adult mortality rate relative to temperature dependent mortality rate at the reference temperature, 0.8, as opposed to the M_pk of the other parameters, 0.8 (Table 5).

Furthermore, the small impact of development time and juvenile mortality, here described in terms of probability of survival, p_{EA}, underlines the degree to which the Parham-Michaels model differs from the Smallwood-Pawar and Amarasekare-Savage models in which development time and juvenile mortality rate, and by extension juvenile survivorship, is indicated to be an important

aspect of the model. This major difference in how the model responds to life history trait related to the juvenile life history stages may be the key driver behind the divergence of the two types of models. While the mechanistic Amarasekare-Savage and Smallwood-Pawar models both explicitly model juvenile survivorship as an exponential decay, under the assumption that disease vectors will exhibit Type III survivorship during juvenile stages, with both the rate of decline, $\bar{z}$, and the period over which the decline occurs, a, modelled as independent parameters based on ecological rates, the Parham-Michaels model describes this process as a probability, bounded between 0 and 1.

As the disease vector population density is such an important parameter in modelling vector-borne disease dynamics (Kuno, 1995; Gage *et al.*, 2008), the choice of model with which to describe the contribution of population density will have a large impact on transmission. Both Parham and Michael (2010) and Mordecai *et al.* (2013) used the Parham-Michaels model in determining the temperature dependence of the basic reproductive rate, R_0, of malaria. From the thermal response curve both studies made predictions about the optimal temperature and the maximum and minimum temperatures for the spread of malaria, with Mordecai *et al.* (2013) notably predicting the optimum temperature of transmission to be substantially lower than had been predicted in previous studies. The large difference in the thermal response curves of population density predicted by the mechanistic Smallwood-Pawar and Amarasekare-Savage models and the Parham-Michaels model indicates that the incorporation fo these models into Dietz's (1993) R_0 model may result in a substantially different prediction. In particular, the much greater thermal tolerance of mosquitoes indicated by the broader thermal response curves predicted by the mechanistic models may result in the range at which the basic reproductive rate is positive, and therefore the disease is able to spread, to be substantially broader than indicated by previous studies. Therefore, a priority in the continuation of this work is the implementation of the mechanistic models into the R_0 model and the assessment of the impact of the differing modelling approaches.

The greater thermal tolerance of disease vectors predicted by the mechanistic models also has important connotations for how climate change is expected to affect disease vectors and therefore the transmission of vector-borne diseases. The broader thermal response curve predicted by the Smallwood-Pawar and Amarasekare-Savage models indicates a lower sensitivity of vector population density to temperature than that predicted by the Parham-Michaels model. The resulting reduction in the predicted thermal sensitivity of disease transmission would result in a reduced impact of changing temperature profiles associated with climate on the distribution and prevalence of vector-borne disease than predicted in studies such as Parham and Michael (2010), which used the Parham-Michaels model to forecast changing R_0 in Tanzania under different climate change scenarios. Differences in the forecasts of the changes in disease dynamics under climate will therefore impact on responses in terms of the socially and humanitarian provisions made to tackle these changes.

Incorporation of the mechanistic models into the R_0 model will also allow for the further examination of the importance of the fecundity schedule. Once incorporated into a second model, the difference in the thermal response curves predicted by the Smallwood-Pawar and Amarasekare-Savage models may not have a significant effect on the thermal response curve for disease transmission. In this context, the Amarasekare-Savage model may be preferable due to its greater simplicity and therefore the lower number of parameters requiring parametrisation. However, the results of this paper suggest that the simplified fecundity schedule of the Amarasekare-Savage model may result in the model being overly sensitive to adult mortality rate. This is important to recognise when

using the sensitivity of these models to assess aspects of mosquito life history on which to focus vector population control methods. Whereas the sensitivity of the Smallwood-Pawar model to development time and juvenile mortality rate indicated by this study strongly suggest that targeting juvenile life stages would have the greatest impact on the population density, it may be concluded from the sensitivity of the Amarasekare-Savage model measures affecting adult mortality rate may be equally effective.

The differences between the models indicated by these results, and the important consequences of these differences, means that it is also important that the quality of the models is determined. In order to determine which approach best describes the observed population dynamics, and therefore ought to be incorporated into the larger framework for studying the dynamics of vector-borne diseases, further work need to be done to validate these models against empirical data and carry out a model selection. Furthermore, model validation and selection can be used to determine whether the assumption made by Amarasekare and Savage (2012) results in a significant loss of accuracy given the degree to which it simplifies the model by comparing measures of fit, such as the Akaike Information Criterion, calculated for the Amarasekare-Savage and Smallwood-Pawar models.

One issue with validating these models, however, is the parametrisation of the necessary life history traits. As described in Supplementary Information II, I attempted to parametrise the models for a dataset of thermal responses of life history traits in disease vectors. However, the data was found to not be of high enough quality due to the low thermal resolution of the majority of studies, resulting in a low number of successful fits of thermal response models. Furthermore, this resulted in there being no high enough quality fits for all the required life history parameters for a single species, let alone for populations for the same location with the same experimental conditions. In addition to the quality of the data, the life history traits required by the mechanistic models do not necessarily reflect those commonly reported in the literature. For example, peak fecundity, b_{pk}, is used by both the Amarasekare-Savage and Smallwood-Pawar model to scale the fecundity schedule. However, this is not a life history trait conventionally reported in the literature and therefore had to be estimated as being approximately equal to the mean fecundity, $\bar{b}$, based on the assumption that the fecundity schedule is so sharply peaked that the mean fecundity is dominated by the peak fecundity (Amarasekare and Savage, 2012). Future work will therefore require further collation of data and also collaboration for experimental ecologists in order to develop a conversation about the requirements of the models as relates to the traits being studied and the resolution of the data.

Similarly, this study was limited in the parametrisation of the equilibrium solution of the logistic growth equation. Without data from which values for the initial population size, M_0, and carrying capacity, K, could be estimated it was not possible to convert the thermal response curves of the population growth rate, r_max, predicted by the Smallwood-Pawar and Amaraseakre-Savage models into a population density in such a way as to allow direct comparison to the population density predicted by the Parham-Michaels model. As the thermal response curves were therefore standardised it was only possible to compare the shape of the curves and the values predicted which may also vary between models.

Conclusion

We have shown that different approaches to modelling the temperature dependence of disease vector population density produce radically different thermal response curves. This has important connotations was the application of temperature dependent models of vector density in disease transmission models or to forecast changes in disease population dynamics under climate change. It is therefore essential that the extent to which these differences impact on our predictions of the dynamics of vector-borne disease. Furthermore, validation of these models is required so as to determine the most appropriate method for modelling vector population density, in order to incorporate the best models into epidemiological models.

References

Altizer, S. Ostfeld, R. S. Johnson, P. T. J. Kutz, S., and Harvell, C. D. (2013), Climate change and infectious diseases: from evidence to a predictive framework. Science (New York, N.Y.), **341**, 514–9.

Amarasekare, P. and Coutinho, R. M. (2013), The intrinsic growth rate as a predictor of population viability under climate warming. Journal of Animal Ecology, **82**, 1240–1253.

Amarasekare, P. and Savage, V. (2012), A framework for elucidating the temperature dependence of fitness. The American naturalist, **179**, 178–91.

Angilletta, M. J. (2009). Thermal adaptation: a theoretical and empirical synthesis. Oxford: Oxford University Press.

Banu, S. Hu, W. Guo, Y. Hurst, C., and Tong, S. (2014), Projecting the impact of climate change on dengue transmission in dhaka, bangladesh. Environment International, **63**, 137–142.

Beck-Johnson, L. M. Nelson, W. A. Paaijmans, K. P. Read, A. F. Thomas, M. B., and Bjø rnstad, O. N. (2013), The effect of temperature on Anopheles mosquito population dynamics and the potential for malaria transmission. PLoS ONE, **8**.

Campbell, L. P. Luther, C. Moo-Llanes, D. Ramsey, J. M. Danis-Lozano, R., and Townsend Peterson, A. (2015), Climate Change Influences on Global Vector Distributions for Dengue and Chikungunya Viruses. Philosophical Transactions of the Royal Society of London B: Biological Sciences, **370**.

Caswell, H. (1989). Matrix population models. Sinauer Associates Associates, Inc., Massachusetts, Massachusetts.

Childers, C. C. Rodrigues, J. C. V., and Welbourn, W. C. (2003), Host plants of brevipalpus californicus, b. obovatus, and b. phoenicis (acari: Tenuipalpidae) and their potential involvement in the spread of viral diseases vectored by these mites. Experimental & applied acarology, **30**, 29–105.

Dell, A. I. Pawar, S., and Savage, V. M. (2011), Systematic variation in the temperature dependence of physiological and ecological traits. Proceedings of the National Academy of Sciences of the United States of America, **108**, 10591–10596.

Dietz, K. (1993), The estimation of the basic reproduction number for infectious diseases. Statistical methods in medical research, **2**, 23–41.

Dommar, C. J. Lowe, R. Robinson, M., and Rodó, X. (2014), An agent-based model driven by tropical rainfall to understand the spatio-temporal heterogeneity of a chikungunya outbreak. Acta Tropica, **129**, 61–73.

Gage, K. L. Burkot, T. R. Eisen, R. J., and Hayes, E. B. (2008), Climate and vectorborne diseases. American journal of preventive medicine, **35**, 436–450.

Gething, P. W. Smith, D. L. Patil, A. P. Tatem, A. J. Snow, R. W., and Hay, S. I. (2010), Climate change and the global malaria recession. Nature, **465**, 342–345.

González, C. Paz, A., and Ferro, C. (2014), Predicted altitudinal shifts and reduced spatial distribution of Leishmania infantum vector species under climate change scenarios in Colombia. Acta Tropica, **129**, 83–90.

Hales, S. de Wet, N. Maindonald, J., and Woodward, A. (2002), Potential effect of population and climate changes on global distribution of dengue fever: an empirical model. The Lancet, **360**, 830 – 834.

Heesterbeek, J. (1996), The concept of R0 in epidemic theory. Statistica Neerlandica, **50**, 89–110.

IPCC. (2013). Fifth Assessment Report. Cambridge: Cambridge University Press, Cambridge, United Kingdom and New York, NY, USA.

Kitajima, E. W. Rezende, J. a. M., and Rodrigues, J. C. V. (2003), Passion fruit green spot virus vectored by Brevipalpus phoenicis (Acari: Tenuipalpidae) on passion fruit in Brazil. Experimental and Applied Acarology, **30**, 225–231.

Kuno, G. (1995), Review of the factors modulating dengue transmission. Epidemiologic reviews, **17**, 321–335.

Lana, R. M. Carneiro, T. G. S. Honório, N. a., and Codeço, C. T. (2014), Seasonal and nonseasonal dynamics of Aedes aegypti in Rio de Janeiro, Brazil: Fitting mathematical models to trap data. Acta Tropica, **129**, 25–32.

Lotka, A. J. (1907), Relation between birth rates and death rates. Science, pages 21–22.

Lotka, A. J. and Sharpe, F. (1911), A problem in age distribution. Philosophical Magazine, **21**, 339–345.

Lysyk, T. J. and Danyk, T. (2007), Effect of temperature on life history parameters of adult culicoides sonorensis (diptera: Ceratopogonidae) in relation to geographic origin and vectorial capacity for bluetongue virus. Journal of medical entomology, **44**, 741–751.

Medone, P. Ceccarelli, S. Parham, P. E., and Rabinovich, J. E. (2015), The impact of climate change on the geographical distribution of two vectors of Chagas disease : implications for the force of infection. Philosophical Transactions of the Royal Society of London B: Biological Sciences, **370**.

Meyrowitsch, D. W. Pedersen, E. M. Alifrangis, M. Scheike, T. H. Malecela, M. N. Magesa, S. M. Derua, Y. a. Rwegoshora, R. T. Michael, E., and Simonsen, P. E. (2011), Is the current decline in malaria burden in sub-Saharan Africa due to a decrease in vector population? Malaria journal, **10**, 188.

Mordecai, E. A. Paaijmans, K. P. Johnson, L. R. Balzer, C. Ben-Horin, T. de Moor, E. McNally, A. Pawar, S. Ryan, S. J. Smith, T. C., and Lafferty, K. D. (2013), Optimal temperature for malaria transmission is dramatically lower than previously predicted. Ecology Letters, **16**, 22–30.

Nault, L. (1997), Arthropod transmission of plant viruses: a new synthesis. Annals of the Entomological Society of America, **90**, 521–541.

Newville, M. Stensitzki, T. Allen, D. B., and Ingargiola, A. (2014). LMFIT: Non-Linear Least-Square Minimization and Curve-Fitting for Python. URL `http://dx.doi.org/10.5281/zenodo.11813`.

Ogden, N. H. Radojević, M. Wu, X. Duvvuri, V. R. Leighton, P. a., and Wu, J. (2014), Estimated effects of projected climate change on the basic reproductive number of the lyme disease vector ixodes scapularis. Environmental Health Perspectives, **122**, 631–638.

Ostfeld, R. S. and Brunner, J. L. (2015), Climate change and Ixodes tick-borne diseases of humans. Philosophical Transactions of the Royal Society of London B: Biological Sciences, **370**.

Parham, P. E. and Michael, E. (2010), Modeling the effects of weather and climate change on malaria transmission. Environmental Health Perspectives, **118**, 620.

Parham, P. E. Waldock, J. Christophides, G. K. Hemming, D. Agusto, F. Evans, K. J. Fefferman, N. Gaff, H. Gumel, A. Ladeau, S. Lenhart, S. Mickens, R. E. Naumova, E. N. Ostfeld, R. S. Ready, P. D. Thomas, M. B. Velasco-hernandez, J., and Michael, E. (2015)*a*, Climate , environmental and socio-economic change : weighing up the balance in vector-borne disease transmission. Philosophical Transactions of the Royal Society of London B: Biological Sciences, **370**.

Parham, P. E. Waldock, J. Christophides, G. K., and Michael, E. (2015)*b*, Climate change and vector-borne diseases of humans. Philosophical Transactions of the Royal Society of London B: Biological Sciences, **370**.

Purse, B. V. Mellor, P. S. Rogers, D. J. Samuel, A. R. Mertens, P. P., and Baylis, M. (2006), Climate change and the recent emergence of bluetongue in europe. Nature Reviews Microbiology, **4**.

R Development Core Team, R. (2011). R: A Language and Environment for Statistical Computing. URL `http://www.r-project.org`.

Rodrigues, J. Kitajima, E. Childers, C., and Chagas, C. (2003), Citrus leprosis virus vectored by brevipalpus phoenicis (acari: Tenuipalpidae) on citrus in brazil. Experimental & applied acarology, **30**, 161–179.

Savage, V. M. Gilloly, J. F. Brown, J. H. Charnov, E. L. Gillooly, J. F., and West, G. B. (2004), Effects of body size and temperature on population growth. The American naturalist, **163**, 429–41.

Schoolfield, R. Sharpe, P., and Magnuson, C. (1981), Non-linear regression of biological temperature-dependent rate models based on absolute reaction-rate theory. Journal of theoretical biology, **88**, 719–731.

Stavrinides, M. C. and Mills, N. J. (2011), Influence of temperature on the reproductive and demographic parameters of two spider mite pests of vineyards and their natural predator. BioControl, **56**, 315–325.

Tabachnick, W. J. (2010), Challenges in predicting climate and environmental effects on vector-borne disease episystems in a changing world. The Journal of experimental biology, **213**, 946–954.

Terblanche, J. S. Clusella-Trullas, S. Deere, J. A., and Chown, S. L. (2008), Thermal tolerance in a south-east african population of the tsetse fly glossina pallidipes (diptera, glossinidae): implications for forecasting climate change impacts. Journal of Insect Physiology, **54**, 114–127.

WHO. (2004). The World health report: 2004: Changing history. Geneva: World Health Organisation.

WHO. (2014). World malaria report 2013. Geneva: World Health Organisation.

WHO Special Programme for Research and Training in Tropical Diseases WHO Department of Control of Neglected Tropical Diseases, and WHO Epidemic and Pandemic Alert. (2009). Dengue: guidelines for diagnosis, treatment, prevention and control. Geneva: World Health Organisation.

Zell, R. (2004), Global climate change and the emergence/re-emergence of infectious diseases. International Journal of Medical Microbiology Supplements, **293**, 16–26.

Supplementary Information I: Derivation of the Smallwood-Pawar Model

In age-structured populations, the expected reproductive success of an individual can be described using the continuous form of the Euler-Lotka equation:

$$\int_{a}^{\infty} \mathrm{e}^{-r_{max}x} l_x b_x \,\mathrm{d}x = 1 \tag{12}$$

where r_{max} is the population growth rate, α is the age of first reproduction, l_x is the age-specific survivorship, and B_x is the age-specific fecundity. This can be solved to give the population growth rate, r_{max}.

As arthropods and especially disease vectors are expected to have a Type III survivorship curve, given an instantaneous mortality rate, z, age-specific survivorship, l_x, declines exponentially with age and can be described thus:

$$l_x = l_a \mathrm{e}^{-z(x-a)} \tag{13}$$

Here, l_a is the proportion of eggs surviving to adulthood (age a). Which, given an instantaneous mortality rate across all juvenile stage, $\bar{z}$, can be modelled thus:

$$l_a = \mathrm{e}^{-\int_0^a z_x \,\mathrm{d}x} = \mathrm{e}^{-\bar{z}a} \tag{14}$$

which, when when substituted into Equation 13, gives:

$$l_x = \mathrm{e}^{-(\bar{z}a + z(x-a))} \tag{15}$$

This may be adapted for a variable mortality rate, for example due to senescence.

With respect to age-specific fecundity, b_x, fecundity is expected to reach a peak, b_{pk}, shortly after maturation and then decline gradually with age, thus taking an asymmetric unimodal shape, which can be described using a rescaled gamma function as shown in Figure something. b_x can thus be modelled as:

$$b_x = b_{pk} \mathrm{e}^{\frac{(k-1)(x-x_{pk})}{a-x_{pk}}} (x-a)^{k-1} (x_{pk}-a)^{1-k} \tag{16}$$

where x_{pk} is the age at which individuals achieve peak fecundity, b_{pk}, and k is the shape parameter in a gamma distribution and controls the spread of the fecundity schedule.

Substituting Equations 15 and 16 into Equation 12 and evaluating the integral produces, after simplification:

$$\mathrm{e}^{k-a\bar{z}-ar_{max}-1} \Gamma(k) b_{pk} (x_{pk}-a)^{1-k} (z + r_{max} + \frac{k-1}{x_{pk}-a})^{-k} = 1 \tag{17}$$

where $\Gamma(.)$ is the gamma function.

Rearranging Equation 17 and taking logarithms of each side gives:

$$ar_{max} + k \log(z + \frac{k-1}{x_{pk}-a} + r_{max}) = \log(\Gamma(k) b_{pk}) - (k-1)\log(x_{pk}-a) + a\bar{z} + k - 1 \tag{18}$$

As this cannot be solved for r_{max} because it lies with a log term on the left-hand side of Equation 18, the log term is approximated using the first two terms of it's power series expansion around

the point $r_{max} = 0$, giving:

$$\log(z + \frac{k-a}{x_{pk}-a} + r_{max}) \approx \log(z + \frac{k-1}{x_{pk}-a}) + \frac{r_{max}(x_{pk}-a)}{z(x_{pk}-a)+k-1} \tag{19}$$

Substituting Equation 19 into Equation 18 and rearranging produces the approximation of r_{max}:

$$r_{max} \approx \left(\log\left(\frac{\Gamma(k)b_{pk}(x_{pk}-a)}{(z(x_{pk}-a)+k-1)^k}\right) - a\bar{z} + k - 1\right)\left(\frac{z(x_{pk}-a)+k-1}{az(x_{pk}-a)-a+kx_{pk}}\right) \tag{20}$$

as given in the main text. This approximation is excellent as long as r_{max} is small (i.e. < 1).

As discussed in the main text, r_{max} is translated into population density using the logistic growth equation:

$$M_t = \frac{M_0 K \mathrm{e}^{r_{max}t}}{K + M_0(\mathrm{e}^{r_{max}t} - 1)} \tag{21}$$

where M_t is the population density, M_0 is the initial population size, and K is the carrying capacity.

Supplementary Information II: Parameter Fitting

Parametrisation

In order to compare the models' predictions, data on the necessary ecological parameters was collated from sources in the literature and from other researchers. The necessary parameters for each of the models included in this study are summarised in Table 6 below.

Table 6: Summary of the parameters included in each model

Model	Parameter	SI units	Description
Pawar	b_{pk}	offspring female^{-1} s-1	Mean greatest reproductive rate
	x_{pk}	s	Mean age at largest reproductive event
	a	s	Mean age of maturation
	z	s^{-1}	Adult mortality rate
	$\bar{z}$	s^{-1}	Mean mortality rate across all juvenile stages
	k		Spread of the fecundity schedule
Amarasekare & Savage	b_{pk}	offspring female^{-1} s-1	Mean greatest reproductive rate
	a	s	Mean age of maturation
	z	s^{-1}	Adult mortality rate
	$\bar{z}$	s^{-1}	Mean mortality rate across all juvenile stages
Parham & Michaels	$\bar{b}$	offspring female^{-1} s-1?	Mean lifetime reproductive rate
	p_{EA}		Egg to adult survival probability
	a	s	Mean development rate across all juvenile stages
	z	s^{-1}	Adult mortality rate

This dataset was standardised by performing any necessary transformations to convert the data into the forms required by the models and converting the values into the SI units specified in 6. Age of maturation was calculated from development rate by taking the inverse, as was mortality rate from longevity. In order to convert adult daily survival probability to adult mortality rate the negative natural logarithm was taken, as described in Mordecai *et al.* (2013), which was then converted from days into seconds.

As some parameters used in the model were not collected in the literature some approximations

also had to be made. As there were no cases of peak fecundity, b_{pk}, being measured this was approximated as being mean fecundity, $\bar{b}$, as the degree to which the fecundity schedule is peaked means that mean fecundity will be dominated by the peak fecundity (Amarasekare and Savage, 2012). Similarly, the age at which peak fecundity occurs was rarely measured. Assuming that the largest reproductive event, and therefore peak fecundity, was the first reproductive event, the age of peak reproduction was calculated as the age at which the first gonotrophic cycle was completed, which was estimated to be the sum of the age at maturation, a, and the mean length of the gonotrophic cycle, as gonotrophic cycle rate was assumed to not vary with age.

Model Fitting

For each case in the data set, the `lmfit` module in Python (Newville *et al.*, 2014) was applied to fit the Schoolfield model (Schoolfield *et al.*, 1981) (Equation 10) and a quadratic model (Equation 22). The default Levenberg-Marquart algorithm was used to perform the fitting, however both the Nelder-Mead and L-BFGS-B algorithms were explored but provided no particular benefits over Levenberg-Marquart and no improvement to quality of fits.

When fitting the Schoolfield model, initial values for the temperature at with the trait value is maximum (T_{pk}) is estimated as the temperature of the trait value in the data for which the trait value is greatest, and allowed to vary within the fitting between 0 - 50°C. The scaling coefficient, B_0, is estimated as the trait value corresponding to the lowest temperature and had no constraints on value during fitting. The activation energy of the model, E_A, and deactivation energy, E_D, were given the initial values of 0.65 and 0.7 respectively; 0.65 being a generally accepted approximation for most biochemical reactions and the expectation that thermal responses due have a left skew and therefore that E_D will be greater than E_A. For both E_A and E_D, both were constrained to be greater than zero (minimum value = 0.00000001) but no maximum limit was set.

For the quadratic model, with the form:

$$B_T = qT^2 + rT + s \tag{22}$$

the parameters q and r where given the initial value of 0, and s was set as equal to the mean of the observed trait values. This meant that the starting point was from the assumption that the parameter was temperature independent, and therefore the thermal response curve would be a flat, linear relationship of value of close to the mean of the observed data. Furthermore, no constraints were placed on these parameters in the fitting as, being a phenomenological model, there are no prior expectations defined limits on the parameter space, as summarised in Table 7.

Table 7: Summary of the parameter settings used for the model fittings in `lmfit`

Model	Parameter	Vary	Initial Value	Maximum	Minimum
Quadratic	q	True	0	None	None
	r	True	0	None	None
	s	True	Mean trait value	None	None
Schoolfield	B_0	True	Minimum trait value	None	None
	T_{pk}	True	Temperature of maximum observed trait value	0°C	50°C
	E_A	True	0.65	0.0000001	None
	E_D	True	0.7	0.0000001	None

Thermal response cases with fewer than three unique temperature values were excluded as they were deemed *a priori* to not provide the resolution to produce an informative fit describing the thermal dependence of a trait. For the thermal response cases for which both models was successfully fitted, the better model was determined based on the Akaike Information Criterion (AIC), the most appropriate metric of model selection in the context of selecting a model with the better

predictive power. In order to remove low quality fits from the analysis, a threshold for the r-squared score of the selected model as imposed, with fits failing to exceed this threshold excluded from further analysis.

Fitting Results

Of 142 thermal response cases, the Levenberg-Marquart algorithm was used to fit the Schoolfield and quadratic models to 111 cases with data for more than 3 unique temperature values. Of these, for only one case was neither model was successfully fitted.

After removing cases for which neither model produced a fit with satisfactory explanatory power of the variation in the data, based on an r-squared threshold of 0.6, 95 thermal response cases remained. Of these, the Schoolfield model was found to have a lower AIC score for 32 cases; the quadratic model having a lower AIC score in the remain 63.

Supplementary Information III: Computational Analysis

With the exception of the model fitting described in Supplementary Information II, all analysis was carried out using the R software environment (R Development Core Team, 2011). All the scripts used in this project can be accessed online via the bitbucket repository
https://bitbucket.org/TRS114/cmeeresearchproject
as can the data and results files.

References

Altizer, S. Ostfeld, R. S. Johnson, P. T. J. Kutz, S., and Harvell, C. D. (2013), Climate change and infectious diseases: from evidence to a predictive framework. Science (New York, N.Y.), **341**, 514–9.

Amarasekare, P. and Coutinho, R. M. (2013), The intrinsic growth rate as a predictor of population viability under climate warming. Journal of Animal Ecology, **82**, 1240–1253.

Amarasekare, P. and Savage, V. (2012), A framework for elucidating the temperature dependence of fitness. The American naturalist, **179**, 178–91.

Angilletta, M. J. (2009). Thermal adaptation: a theoretical and empirical synthesis. Oxford: Oxford University Press.

Banu, S. Hu, W. Guo, Y. Hurst, C., and Tong, S. (2014), Projecting the impact of climate change on dengue transmission in dhaka, bangladesh. Environment International, **63**, 137–142.

Beck-Johnson, L. M. Nelson, W. A. Paaijmans, K. P. Read, A. F. Thomas, M. B., and Bjø rnstad, O. N. (2013), The effect of temperature on Anopheles mosquito population dynamics and the potential for malaria transmission. PLoS ONE, **8**.

Campbell, L. P. Luther, C. Moo-Llanes, D. Ramsey, J. M. Danis-Lozano, R., and Townsend Peterson, A. (2015), Climate Change Influences on Global Vector Distributions for Dengue and Chikungunya Viruses. Philosophical Transactions of the Royal Society of London B: Biological Sciences, **370**.

Caswell, H. (1989). Matrix population models. Sinauer Associates Associates, Inc., Massachusetts, Massachusetts.

Childers, C. C. Rodrigues, J. C. V., and Welbourn, W. C. (2003), Host plants of brevipalpus californicus, b. obovatus, and b. phoenicis (acari: Tenuipalpidae) and their potential involvement in the spread of viral diseases vectored by these mites. Experimental & applied acarology, **30**, 29–105.

Dell, A. I. Pawar, S., and Savage, V. M. (2011), Systematic variation in the temperature dependence of physiological and ecological traits. Proceedings of the National Academy of Sciences of the United States of America, **108**, 10591–10596.

Dietz, K. (1993), The estimation of the basic reproduction number for infectious diseases. Statistical methods in medical research, **2**, 23–41.

Dommar, C. J. Lowe, R. Robinson, M., and Rodó, X. (2014), An agent-based model driven by tropical rainfall to understand the spatio-temporal heterogeneity of a chikungunya outbreak. Acta Tropica, **129**, 61–73.

Gage, K. L. Burkot, T. R. Eisen, R. J., and Hayes, E. B. (2008), Climate and vectorborne diseases. American journal of preventive medicine, **35**, 436–450.

Gething, P. W. Smith, D. L. Patil, A. P. Tatem, A. J. Snow, R. W., and Hay, S. I. (2010), Climate change and the global malaria recession. Nature, **465**, 342–345.

González, C. Paz, A., and Ferro, C. (2014), Predicted altitudinal shifts and reduced spatial distribution of Leishmania infantum vector species under climate change scenarios in Colombia. Acta Tropica, **129**, 83–90.

Hales, S. de Wet, N. Maindonald, J., and Woodward, A. (2002), Potential effect of population and climate changes on global distribution of dengue fever: an empirical model. The Lancet, **360**, 830 – 834.

Heesterbeek, J. (1996), The concept of R0 in epidemic theory. Statistica Neerlandica, **50**, 89–110.

IPCC. (2013). Fifth Assessment Report. Cambridge: Cambridge University Press, Cambridge, United Kingdom and New York, NY, USA.

Kitajima, E. W. Rezende, J. a. M., and Rodrigues, J. C. V. (2003), Passion fruit green spot virus vectored by Brevipalpus phoenicis (Acari: Tenuipalpidae) on passion fruit in Brazil. Experimental and Applied Acarology, **30**, 225–231.

Kuno, G. (1995), Review of the factors modulating dengue transmission. Epidemiologic reviews, **17**, 321–335.

Lana, R. M. Carneiro, T. G. S. Honório, N. a., and Codeço, C. T. (2014), Seasonal and nonseasonal dynamics of Aedes aegypti in Rio de Janeiro, Brazil: Fitting mathematical models to trap data. Acta Tropica, **129**, 25–32.

Lotka, A. J. (1907), Relation between birth rates and death rates. Science, pages 21–22.

Lotka, A. J. and Sharpe, F. (1911), A problem in age distribution. Philosophical Magazine, **21**, 339–345.

Lysyk, T. J. and Danyk, T. (2007), Effect of temperature on life history parameters of adult culicoides sonorensis (diptera: Ceratopogonidae) in relation to geographic origin and vectorial capacity for bluetongue virus. Journal of medical entomology, **44**, 741–751.

Medone, P. Ceccarelli, S. Parham, P. E., and Rabinovich, J. E. (2015), The impact of climate change on the geographical distribution of two vectors of Chagas disease : implications for the force of infection. Philosophical Transactions of the Royal Society of London B: Biological Sciences, **370**.

Meyrowitsch, D. W. Pedersen, E. M. Alifrangis, M. Scheike, T. H. Malecela, M. N. Magesa, S. M. Derua, Y. a. Rwegoshora, R. T. Michael, E., and Simonsen, P. E. (2011), Is the current decline in malaria burden in sub-Saharan Africa due to a decrease in vector population? Malaria journal, **10**, 188.

Mordecai, E. A. Paaijmans, K. P. Johnson, L. R. Balzer, C. Ben-Horin, T. de Moor, E. McNally, A. Pawar, S. Ryan, S. J. Smith, T. C., and Lafferty, K. D. (2013), Optimal temperature for malaria transmission is dramatically lower than previously predicted. Ecology Letters, **16**, 22–30.

Nault, L. (1997), Arthropod transmission of plant viruses: a new synthesis. Annals of the Entomological Society of America, **90**, 521–541.

Newville, M. Stensitzki, T. Allen, D. B., and Ingargiola, A. (2014). LMFIT: Non-Linear Least-Square Minimization and Curve-Fitting for Python. URL `http://dx.doi.org/10.5281/zenodo.11813`.

Ogden, N. H. Radojević, M. Wu, X. Duvvuri, V. R. Leighton, P. a., and Wu, J. (2014), Estimated effects of projected climate change on the basic reproductive number of the lyme disease vector ixodes scapularis. Environmental Health Perspectives, **122**, 631–638.

Ostfeld, R. S. and Brunner, J. L. (2015), Climate change and Ixodes tick-borne diseases of humans. Philosophical Transactions of the Royal Society of London B: Biological Sciences, **370**.

Parham, P. E. and Michael, E. (2010), Modeling the effects of weather and climate change on malaria transmission. Environmental Health Perspectives, **118**, 620.

Parham, P. E. Waldock, J. Christophides, G. K. Hemming, D. Agusto, F. Evans, K. J. Fefferman, N. Gaff, H. Gumel, A. Ladeau, S. Lenhart, S. Mickens, R. E. Naumova, E. N. Ostfeld, R. S. Ready, P. D. Thomas, M. B. Velasco-hernandez, J., and Michael, E. (2015)*a*, Climate , environmental and socio-economic change : weighing up the balance in vector-borne disease transmission. Philosophical Transactions of the Royal Society of London B: Biological Sciences, **370**.

Parham, P. E. Waldock, J. Christophides, G. K., and Michael, E. (2015)*b*, Climate change and vector-borne diseases of humans. Philosophical Transactions of the Royal Society of London B: Biological Sciences, **370**.

Purse, B. V. Mellor, P. S. Rogers, D. J. Samuel, A. R. Mertens, P. P., and Baylis, M. (2006), Climate change and the recent emergence of bluetongue in europe. Nature Reviews Microbiology, **4**.

R Development Core Team, R. (2011). R: A Language and Environment for Statistical Computing. URL `http://www.r-project.org`.

Rodrigues, J. Kitajima, E. Childers, C., and Chagas, C. (2003), Citrus leprosis virus vectored by brevipalpus phoenicis (acari: Tenuipalpidae) on citrus in brazil. Experimental & applied acarology, **30**, 161–179.

Savage, V. M. Gilloly, J. F. Brown, J. H. Charnov, E. L. Gillooly, J. F., and West, G. B. (2004), Effects of body size and temperature on population growth. The American naturalist, **163**, 429–41.

Schoolfield, R. Sharpe, P., and Magnuson, C. (1981), Non-linear regression of biological temperature-dependent rate models based on absolute reaction-rate theory. Journal of theoretical biology, **88**, 719–731.

Stavrinides, M. C. and Mills, N. J. (2011), Influence of temperature on the reproductive and demographic parameters of two spider mite pests of vineyards and their natural predator. BioControl, **56**, 315–325.

Tabachnick, W. J. (2010), Challenges in predicting climate and environmental effects on vector-borne disease episystems in a changing world. The Journal of experimental biology, **213**, 946–954.

Terblanche, J. S. Clusella-Trullas, S. Deere, J. A., and Chown, S. L. (2008), Thermal tolerance in a south-east african population of the tsetse fly glossina pallidipes (diptera, glossinidae): implications for forecasting climate change impacts. Journal of Insect Physiology, **54**, 114–127.

WHO. (2004). The World health report: 2004: Changing history. Geneva: World Health Organisation.

WHO. (2014). World malaria report 2013. Geneva: World Health Organisation.

WHO Special Programme for Research and Training in Tropical Diseases WHO Department of Control of Neglected Tropical Diseases, and WHO Epidemic and Pandemic Alert. (2009). Dengue: guidelines for diagnosis, treatment, prevention and control. Geneva: World Health Organisation.

Zell, R. (2004), Global climate change and the emergence/re-emergence of infectious diseases. International Journal of Medical Microbiology Supplements, **293**, 16–26.